SPATIALLY RESOLVED TRAPPING DETECTION AND CORRELATION WITH MATERIAL QUALITY IN MULTICRYSTALLINE SILICON

M.C. Schubert[1], S. Riepe[2], and W. Warta[2]

[1]Freiburger Materialforschungszentrum FMF, Stefan-Meier-Str. 21, 79104 Freiburg, Germany
email: martin.schubert@fmf.uni-freiburg.de
[2]Fraunhofer ISE, Heidenhofstr. 2, 79110 Freiburg, Germany,

ABSTRACT: We present images of the total trap density in standard industrial material which are extracted from Carrier Density Imaging (CDI/ILM) measurements. We demonstrate the influence of high temperature on the trap distribution as well as the spatial correlation of traps and crystal defect density. From these observations we deduce that the trapping effect may originate from impurities located at crystal defects. Fast trapping measurements on as-cut wafers are presented that may be used to predict the diffusion length distribution of the processed solar cell for a given cell process. This prediction may be very useful for inline characterisation of starting material.
Keywords: Experimental Methods, Trapping, Diffusion Length

1 INTRODUCTION

Trapping of charge carriers has been presented as a means to characterise material quality [1,2]. In these previous publications the integral trap density of different material has been extracted from photoconductance lifetime measurements averaged over a larger detection area. Correlation between trap density and boron-impurity-contamination has been found as well as correlation with the (integral) crystal defect density. Recently, hydrogen passivation has been correlated with trap density [3]. The most important restriction of these measurements is the lack of spatial resolution which is necessary for examining variations in material quality. Trap images for multicrystalline silicon were reported in [4], recently for Cz-silicon in [5] and analysed for multicrystalline silicon in more detail in [6-9]. The determination of the total trap density from lifetime images has been named as ITM (Infrared Trap Mapping) in [5]. The information about the spatial distribution of trap centres is of high importance for multicrystalline material as we will show in this paper.

We present images of the trap density in multicrystalline silicon obtained from injection dependent lifetime images with Carrier Density Imaging CDI [10,11] (equivalently termed Infrared Lifetime Mapping ILM [12]). The evaluation assumes, that the anomalous increase of apparent lifetime at low injection is caused by a trapping effect. The Hornbeck and Haynes trapping model is used to fit injection dependent measurements for each image pixel.

We examine the effect of high temperature treatment on the distribution of traps. We compare trap density images of a sample before and after a thermal treatment at 880 °C for one hour under argon atmosphere as well as the corresponding recombination lifetime images. Furthermore, we compare trap density images and crystal defect density images for multicrystalline material.

Finally, we correlate trap images on as-cut multicrystalline wafers with diffusion length images obtained using Spectrally Resolved Light Beam Induced Current (SR-LBIC) [13] on finished solar cells processed on adjacent wafers. This correlation may be used to predict the distribution of diffusion length on the finished cell from a fast trap measurement for a given cell process. Trap images may be obtained within a short measurement time in the order of one second and no wafer preparation is needed. Thus, the acquisition of trap images may be used for inline characterisation of starting material.

2 IMAGING OF SPATIALLY RESOLVED TRAP DENSITY

The anomalous increase of apparent lifetime under low-injection conditions may be explained by different models. For a detailed discussion we refer to [6]. In this paper we apply the Hornbeck and Haynes model [14] which assumes a defect level with asymmetric capture cross sections to be responsible for the trapping effect. Free minority carriers are easily captured in these defect states but do not recombine with holes because of the small capture cross sections of these states. In steady-state measurements the minority carrier density is determined by the generation and recombination rate and does not depend on temporary trapping of minority carriers. However, lifetime measurements like QSSPC [15] and CDI/ILM depend on both, the free excess minority and free excess majority carrier density, and assume equality of both. In presence of trapped charges this assumption does not hold because charge neutrality forces the free excess majority carrier density to exceed the free excess minority carrier density. Especially under low-injection conditions this results in an anomalous, increased “apparent” lifetime.

The measured apparent lifetime $\tau_{app}(\Delta n_{app})$ is modelled with the following equations deduced from the Hornbeck and Haynes model. In the case of p-type we find [4]

$$\tau_{app}(\Delta n) = \frac{1}{\alpha_n + \alpha_p} \tau_{rec}(\Delta n) \left[\alpha_n + \alpha_p \left(1 + \frac{n_T(\Delta n)}{\Delta n} \right) \right] \quad (1)$$

$$\Delta n_{app}(\Delta n) = \frac{1}{\alpha_n + \alpha_p} \Delta n \left[\alpha_n + \alpha_p \left(1 + \frac{n_T(\Delta n)}{\Delta n} \right) \right], \quad (2)$$

where $\alpha_{n,p}$ are the absorption coefficients for electrons and holes, τ_{rec} is the low-injection recombination lifetime, Δn is the excess minority carrier density, and n_T is the density of trapped minority carriers with

$$n_T = \frac{N_T \Delta n}{\Delta n + N_T(\tau_t / \tau_g)}. \qquad (3)$$

N_T denotes the total trap density and (τ_t/τ_g) is the trap-escape ratio (see [1] for details). The case of n-type material is analogous.

From equation (1) to (3) an expression for $\tau_{app}(\Delta n_{app})$ can be deduced which is then fitted to injection dependent CDI measurements for each image pixel (see Fig. 1). N_T is used as a fitting parameter and is then displayed. For further details, see [6].

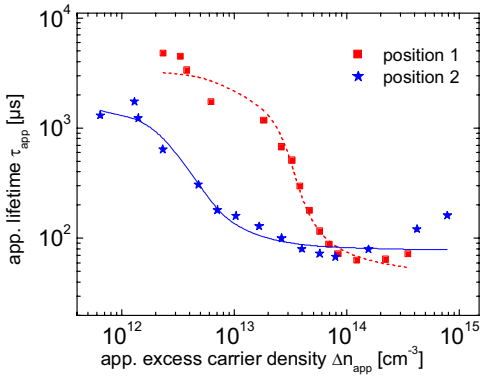

Figure 1: Examples of lifetimes measured with injection dependent CDI under low-injection conditions for different positions on the wafer. The lines indicate the model with adapted trapping parameters.

3 COMPARISON OF TRAP DENSITY AND RECOMBINATION LIFETIME BEFORE AND AFTER HIGH TEMPERATURE STEP

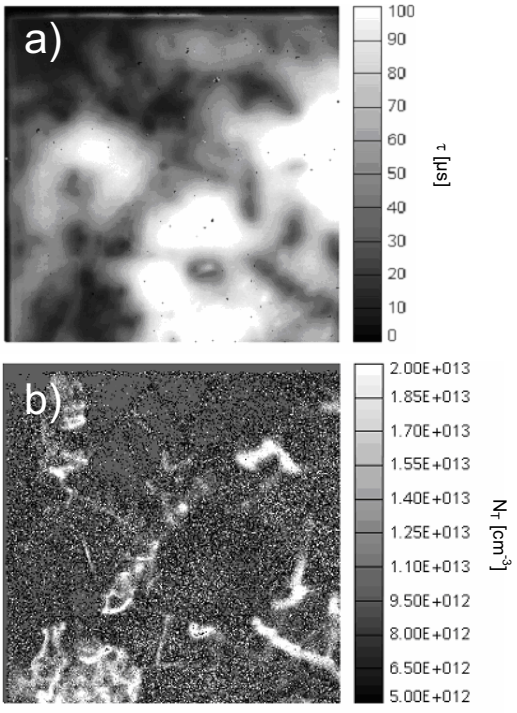

Figure 2: a) Lifetime image of an as grown SiN-passivated multicrystalline silicon sample (12x12mm²) at 1 sun illumination. b) Corresponding total trap density image.

Injection dependent lifetime images have been obtained from standard, directionally solidified multicrystalline silicon samples (12 mm x 12 mm, SiN-passivated) and trap density images have been calculated from these measurements (see Fig. 2). After the measurement, the SiN-passivation has been removed and the samples were heated to 880 °C for 1 hour under Argon atmosphere. After the thermal treatment, the samples have been re-passivated. Again, lifetime and trap density images have been taken (see Fig. 3).

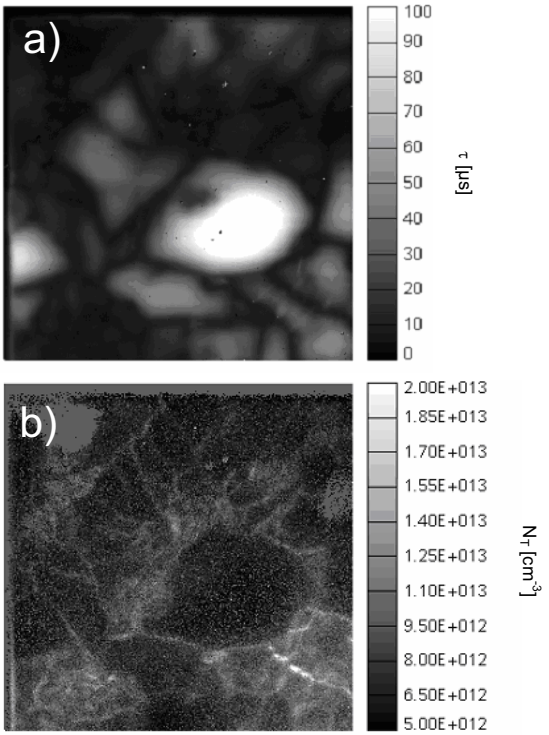

Figure 3: a) Lifetime image of sample shown in Fig. 2 after thermal treatment at 1 sun illumination. b) Corresponding total trap density image.

A re-distribution and reduction of the highest trapping centre concentrations found in the as grown material by the heat treatment may be inferred from these measurements. Nevertheless, the general structure of the trap distribution remains unaffected by the high temperature step.

4 CORRELATION OF TRAP DENSITY AND CRYSTAL DEFECT DENSITY

The trap density image has been compared to an Etch Pit Density EPD measurement on the same material as above (no thermal treatment) (Fig. 4). The crystal defect density is obtained by the following procedure: The surface of the sample under test is polished before Secco-etching the surface. Etch pits are

counted automatically with a microscope and are evaluated to obtain the crystal defect density.

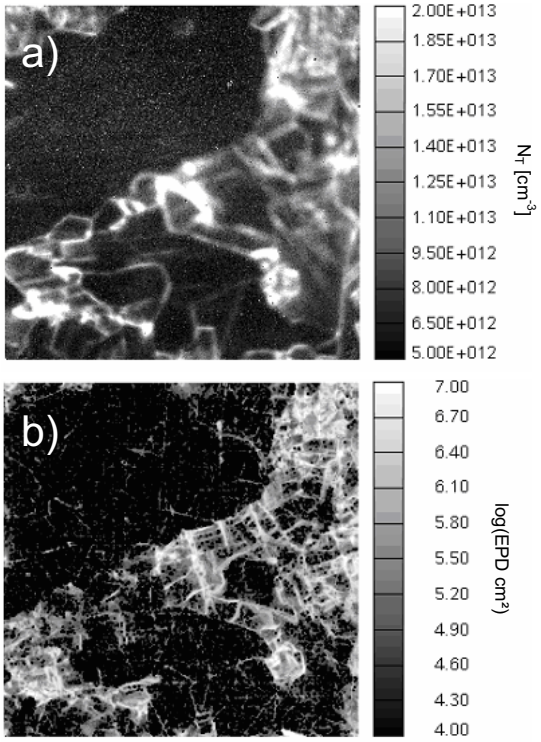

Figure 4: a) Total trap density image (12x12 mm²) b) Crystal defect density from EPD measurement on adjacent wafer.

The distribution of the total trap density correlate very well with the crystal defect density. Even small details in the trap density map correspond to increased crystal defect density. Some additional characteristics in the crystal defect density map are due to scratches induced by the polishing procedure.

The correlation of trapping and crystal defects in combination with the observed influence of high temperature steps on trapping suggests that the trapping effect may be related to impurities which are agglomerated at crystal defects. High temperature may induce diffusion of these impurities leading to two effects: (i) out-diffusion of impurities from regions with very high impurity concentration may be derived from the measurement, and (ii) impurities may diffuse towards crystal defects which were not decorated with these impurities to this extent before.

Bail et al. showed in [16] that silicon nitride passivation layers may be responsible for an increased apparent lifetime under low-injection conditions due to an induced inversion layer. This effect is known as Depletion Region Modulation DRM which has been published also for the case of p-n-junctions by Neuhaus et al. [17]. We measured the apparent lifetime of a sample made from the same material as in the experiments above under low injection (0.008 suns) before and after removal of the silicon nitride passivation layer (Fig. 5). The absolute measured lifetime is lower without SiN-layer which results from surface recombination effects or removal of a minor DRM effect on the full sample area, but the same prominent structures are visible. Thus, the modelled total trap density is not dominated by a DRM effect of the surface.

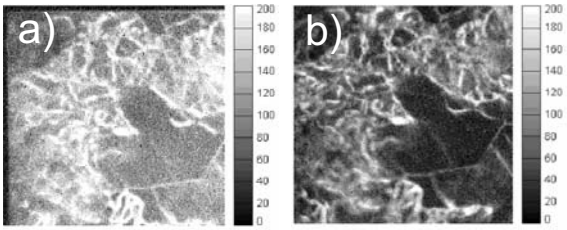

Figure 5: Lifetime measurement [µs] under low injection (0.008 suns) with SiN-passivation layer (a) and without surface passivation (b).

5 CORRELATION OF TRAPPING IMAGE AND DIFFUSION LENGTH

CDI images of the material under test in this paper are dominated by trapping effects at very low injection. Trap images can therefore be obtained directly from one single measurement, if the quantitative calculation of the total trap density is not needed. The low-injection regime can easily be realised, if the wafer is not passivated. Due to high surface recombination the free excess carrier density is low at an illumination of 1 sun. Even for high-lifetime material the free excess carrier density Δn is typically below $3 \cdot 10^{13}$ cm^{-3} (wafer thickness $d \leq 300$ µm) at 1 sun.

Low-injection CDI trap images on as-cut material without any surface preparation have been compared to diffusion length measurements obtained with SR-LBIC on solar cells made from adjacent wafers. Trap image and diffusion length map have been compared at various positions. The trap image values have been plotted versus the diffusion length at these positions in Fig. 6. Examples taken from wafers cut from the bottom region of an ingot and from the middle part of an ingot are shown.

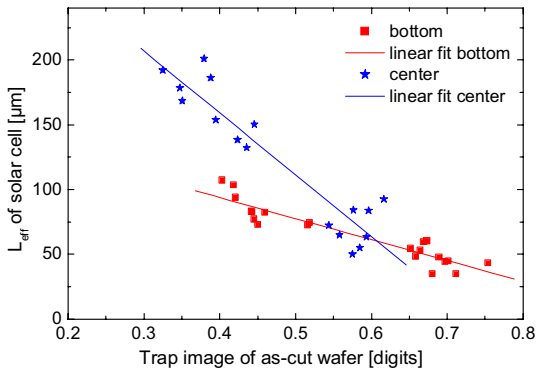

Figure 6: Correlation of trap image of as-cut wafer and L_{eff}-map of finished solar cell for various points. Examples for bottom and centre region of ingot.

Linear fits of this correlation yield a relation which can be used to calculate a spatially resolved prediction of

the diffusion length distribution of the solar cell, with emphasis on the limiting low-quality areas, directly from the trap image (Fig. 7).

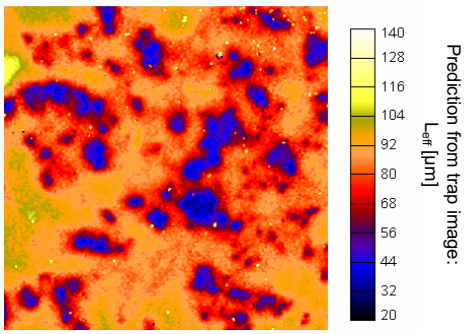

Figure 7: Prediction of L_{eff}-distribution on finished solar cell for a given process from trap image on as-cut wafer.

The prediction of diffusion length correlates well with the SR-LBIC measurement shown in Fig. 8. All regions with low diffusion length may be relocated in the trap image. The slightly increased measurement values in the SR-LBIC measurement on the left side of the cell are most likely due to measurement artefacts.

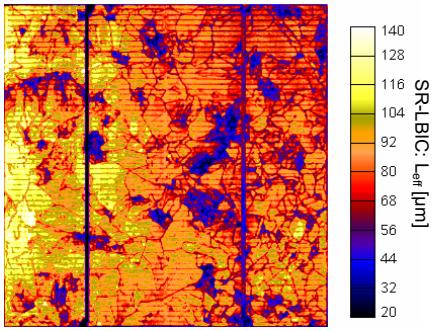

Figure 8: SR-LBIC diffusion length (L_{eff}) map of finished solar cell.

It has to be stressed that this kind of prediction may only be valid for a well defined process on comparable material since diffusion length significantly depends on various process parameters in a complex manner. Nevertheless, the analysis of trap images of as-cut material has a great potential to be a very valuable method to estimate the cell results from measurements of starting material.

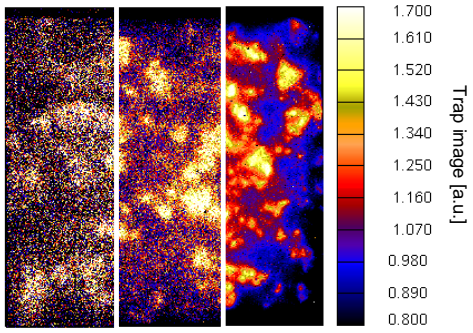

Figure 9: Trap image of wafer examined in Fig. 7 composed of measurements with measurement time of approximately 280 ms, 1 s, and 9 min, from left to right.

Although the measurement time of the presented trap images was several minutes for the images presented in order to achieve high quality, good results can as well be obtained in one second, which is shown in Fig. 9. Measurement times of 280 ms, 1 s, and 9 min are compared for adjacent parts of the wafer shown in Fig. 7. The result with a measurement time of 280 ms already allows to distinguish areas of high and low trap density. The measurement with 1 s measurement time clearly shows detailed differences of trap density.

6 CONCLUSION

Images of the total trap density from CDI/ILM measurements are presented. An influence of a high temperature treatment on the spatial distribution of traps is reported as well as a correlation of crystal defect density and trap density. A fast trap characterisation method is proposed which may be used to predict the diffusion length of the finished solar cell from a measurement on the as-cut wafer for a given cell process.

7 ACKNOWLEDGEMENT

We thank H. Lautenschlager for sample processing and F. Heinz for help with the measurements. This work was supported by the German Federal Ministry of Education and Research (BMBF) within the framework of the “Netz Diagnostik” project under the contract number 01SF0401.

[1] D. Macdonald, A. Cuevas, Appl. Phys. Lett. **74** (12), 1710 (1999)
[2] D. Macdonald, A. Cuevas, Solar Energy Mat. & Solar Cells, **65,** 509, (2001)
[3] H.F.W. Dekkers, L. Carnel, and G. Beaucarne, Appl. Phys. Lett. **89**, 013508 (2006)
[4] M.C. Schubert, J. Isenberg, S. Rein, S. Bermejo, S.W. Glunz, W. Warta, 20th EU-PVSC, Barcelona (2005)
[5] P. Pohl, J. Schmidt, K. Bothe, R. Brendel, Appl. Phys. Lett. **87** 142104 (2005)
[6] M.C. Schubert, S. Riepe, S. Bermejo, W. Warta, J. Appl. Phys. **99**, 114908 (2006)

[7] M.C. Schubert, W. Warta, Silicon Forest Workshop, Falkau (2006)
[8] P. Pohl, Silicon Forest Workshop, Falkau (2006)
[9] P. Pohl, J. Schmidt, K. Bothe, R. Brendel, 4th WCPEC, Hawaii (2006)
[10] S. Riepe, J. Isenberg, C. Ballif, S.W. Glunz, W. Warta, Proc. 17th EC-PVSC, Munich, 1597 (2001)
[11] M.C. Schubert, J. Isenberg, W. Warta, J. Appl. Phys., 94 (6), 4139 (2003)
[12] M. Bail, J. Kentsch, R. Brendel, M. Schulz, Proc. 28th IEEE-PVSC, Anchorage, 99 (2000)
[13] W. Warta, J. Sutter, R. Schindler, B.F. Wagner, 2nd PVSEC, Vienna, Austria 1650, (1998)
[14] J.A. Hornbeck, J.R. Haynes, Phys. Rev. **97**, 311 (1955)
[15] R. Sinton, A. Cuevas, M. Stuckings, Proc. 25th IEEE-PVSC, Washington, 457 (1996)
[16] M. Bail, J. Kentsch, R. Brendel, M. Schulz, Proc. 28th IEEE-PVSC, Anchorage, 99 (2000)
[17] D.H. Neuhaus, P.J. Cousins, A.G. Aberle , 3rd WCPEC, Osaka, 91, (2003)